Iranian Journal of Basic Medical Sciences

ijbms.mums.ac.ir

IJBMS

Hypericin-photodynamic therapy inhibits proliferation and induces apoptosis in human rheumatoid arthritis fibroblast-like synoviocytes cell line MH7A

Kun Zhang [1], Shan Gao [2], JiaYi Guo [3], GuoHua Ni [1], Zhe Chen [3], Feng Li [3], XiaoLei Zhu [3], YongBing Wen [3], YanXing Guo [3*]

[1] Department of Orthopedics, No. 91 Central hospital of Liberation Army, Jiaozuo 454150, Henan province, China
[2] Faculty of Graduate Studies, Hunan University of Chinese Medicine, Changsha 410208, Hunan Province, China
[3] Department of Orthopedics, Luoyang Orthopedic Hospital of Henan Province, Luoyang 471000, Henan Province, China

ARTICLE INFO

Article type:
Original article

Article history:
Received: May 27, 2017
Accepted: Sep 28, 2017

Keywords:
Apoptosis
Fibroblast-like synoviocyte
Hypericin-photodynamic -therapy
Nuclear factor kappa-B
Rheumatoid arthritis
Reactive oxygen species

ABSTRACT

Objective(s): To elucidate the effects and potential mechanisms of hypericin-photodynamic therapy (HYP-PDT) for treating the human rheumatoid arthritis (RA) fibroblast-like synoviocyte (FLS) MH7A cell-line.

Materials and Methods: MH7A cells were subjected to HYP-PDT intervention and apoptosis was evaluated via MTT, nuclear staining, and flowcytometry analyses. Intracellular reactive oxygen species (ROS) were measured with the fluorescent probe 2′7′-dichlorofluorescein diacetate (DCFH-DA). To verify the effects of HYP on apoptotic and nuclear factor kappa-B (NF-κB) pathways, caspase-8, 9, poly-ADP-ribose polymerase (PARP), phosphorylated (p)-NF-κB p65, NF-κB p65 and p-IκBα protein expressions were quantified with Western blot. Quantitative real-time PCR was used to assay NF-κB p65 mRNA.

Results: HYP-PDT inhibited MH7A cell viability and induced apoptosis in a dose-dependent manner. Meanwhile, intracellular ROS levels increased significantly after HYP-PDT treatment. Furthermore, the expression of cleaved caspase-9 and PARP was increased by HYP-PDT treatment, with a concurrent decline in NF-κB.

Conclusion: HYP-PDT induces apoptosis in MH7A cells, at least partially, via generation of ROS, regulation of the apoptotic pathway and suppression of the NF-κB pathway. These findings suggest that HYP-PDT may be a potential treatment for RA.

► *Please cite this article as:*
Zhang K, Gao Sh, Guo JY, Ni GH, Chen Zh, Li F, Zhu XL, Wen YB, Guo YX. Hypericin-photodynamic therapy inhibits proliferation and induces apoptosis in human rheumatoid arthritis fibroblast-like synoviocytes cell line MH7A. Iran J Basic Med Sci 2018; 21:130-137.

Introduction

Rheumatoid arthritis (RA) is a systemic autoimmune disorder characterized by inflammation of synovial tissues and progressive erosion of adjacent cartilage and subchondral bone, which subsequently causes irreparable joint destruction (1-3). The pathological process of RA is marked primarily by the invasive growth of inflamed and aberrant hyperplastic synovial tissue into articular cartilage and bone. Thus, excessive inflammatory cytokines and proteolytic enzymes are released from RA fibroblast-like synoviocytes (FLS) in hyperplastic synovial tissue, resulting in degradation and destruction of cartilage and subchondral bone (4, 5). Although mechanisms underlying hyperplastic synovitis are not completely understood, insufficient apoptosis may contribute to the pathogenesis of RA (6). Recently, accumulating evidence suggests that resistance to apoptosis promotes synovial hyperplasia and is linked closely to the invasive and tumor-like phenotype of RA-FLS (7). Therefore, production of inflammatory mediators and tumor-like growth of RA-FLS due to insufficient apoptosis are considered pathological hallmarks of RA (8), and thus may be a potential therapeutic target for controlling the inflammatory response and modulating apoptosis in RA-FLS.

Photodynamic therapy (PDT) is considered a minimally invasive, site-specific modality (9) for treating diseases such as cancer. Additionally, many studies suggest that PDT may be used to treat RA (10, 11), given its ability to limit the abnormal proliferation of synovial tissue, such as that seen in RA patients (9). Studies indicate that PDT employs a mechanism that differs from those of radiotherapy and chemotherapy, increasing the apoptotic potential of cells resistant to more conventional treatments (9). Moreover, PDT can recognize and selectively destroy cancer cells with no adverse impact on normal cells (12). PDT consists of a photosensitizer, molecular oxygen, and external visible light at a specific wavelength (13). The photosensitizer is critical for effective treatment as it

*Corresponding author: Yanxing Guo. Department of Orthopedics, Luoyang Orthopedic Hospital of Henan Province, Luoyang, Henan, 471000, China. Tel: +86-18553354680; email: 18553354680@163.com

reacts with molecular oxygen to produce cytotoxic reactive oxygen species (ROS) (14), which are toxic to the target tissue by oxidizing cellular organelle membranes, and interfering with cellular signal pathways, leading to apoptosis or necrosis and eventually destroying diseased tissue (14). Current studies have focused on identifying satisfactory photosensitizer drugs, given that drugs such as hematoporphyrin and its derivatives have long half-lives that cause complications limiting their clinical applications (15).

Hypericin (HYP), a polycyclic quinone, is a naturally occurring photosensitizer extracted from *Hyperforin perforatum* (St. John's wort) (16). For decades, HYP has been used as a drug treatment for depression and viral infections. Furthermore, due to its light-dependent activity (17-19), HYP is also one of the most potent photosensitizers that has a maximum absorption peak of ~599 nm (20) and exhibits several advantages over other photosensitizers. For example, HYP has substantial quantum yield, intense absorption spectrum in the visible region, low photo bleaching, short half-life (27 hr even at a dosage of 1500 μg/kg), and a wide excitation range (21, 22). Recently, there has been growing interest in HYP-PDT as a potential treatment for various cancers (23). Several studies have demonstrated that HYP-PDT has high tumor specific cytotoxicity and minimal side effects (24, 25). Furthermore, HYP-PDT can induce vascular injury in tumor cell models through inhibition of mitochondrial function, and can induce apoptosis in cancer cells through activation of the caspase-dependent pathway (26). Based on this background, we sought to explore whether the therapeutic potential of HYP-PDT in cancer treatment extends to RA, which is characterized by invasive and tumor-like hyperplastic synovium due to insufficient apoptosis of RA-FLS. To the best of our knowledge, no studies have described the effects of HYP-PDT on RA *in vivo* or *in vitro;* therefore, we offer an initial report regarding potential mechanisms of HYP-PDT for treating RA.

Specifically, we used HYP-PDT to treat an MH7A cell model of RA-FLS and studied how HYP induces photocytotoxicity (27). Our data showed that HYP-PDT inhibited MH7A cell proliferation, induced apoptosis, and upregulated intracellular ROS in a dose-dependent manner. Apoptotic and nuclear factor kappa-B (NF-κB) pathways were also modulated by HYP-PDT treatment, suggesting potential therapeutic promise for HYP-PDT to treat human RA.

Materials and Methods

Reagents

Human RA-FLS MH7A cell line was obtained from Enzyme Research Technology (Shanghai, China). Hypericin was purchased from Jingzhu Technology (Nanjing, China). Antibodies against caspase-8, caspase-9, cleaved caspase-9, poly-ADP-ribose polymerase (PARP), cleaved PARP, p-NF-κB p65, NF-κB p65, p-IκBα, and β-actin were purchased from Cell Signaling Technology (Boston, MA, USA). Primers for NF-κB p65 were designed and synthesized by Sangon Biotech (Shanghai, China).

Cell lines and cell culture

MH7A cells (27) were cultured in DMEM/HIGH Glucose medium (Hyclone, Logan, UT, USA), supplemented with 10% fetal bovine serum (FBS; Gibco Life Technologies, Carlsbad, CA, USA) and 1% penicillin/streptomycin (Sigma-Aldrich, St. Louis, MO, USA), in a CO_2 incubator at 37 °C, 5% CO_2 and saturated humidity environment.

In vitro HYP-PDT treatment

PDT was performed on MH7A cells according to previously published guidelines (28). Briefly, cells were pre-incubated for 24 hr and culture medium was removed and exchanged with fresh medium containing HYP (0, 0.25, 0.5, 1, 2 and 4 μM). Then, cells were cultured for another 1 hr in the dark. Subsequently, cells were exposed to 593 nm wavelength monochromatic homemade diode irradiation to give a light energy dose of 1.5 J/cm^2. Next, cells were incubated for 24 hr in the dark. MH7A cell controls were treated in a similar manner but without HYP induction.

Cell viability assays

A 3-(4, 5-dimethylthiazol-2-yl)-2,5-diphenyltetrazolium bromide (MTT) assay was used to measure cytotoxicity of HYP (29). Approximately, 5 × 10^3 cells were seeded in 2 separate 96-well plates and cultured for 24 hr. Then, cells were treated with fresh medium containing HYP (0–4 μM) for 1 hr in the dark. Next, cells were treated with or without light irradiation (593 nm monochromatic homemade diode irradiation; 1.5 J/cm^2). After interventions, cells were incubated for an additional 24 hr in the dark. Afterwards, 20 μl of MTT reagent (5 mg/ml) was added to the wells, and cells were incubated for 4 hr in the dark. Liquid was removed and 150 μl DMSO was added with shaking for 15 min in the dark. Finally, absorption was read and recorded using a microplate reader (BioTek, Winooski, VT, USA). Cell viability was measured relative to the untreated cells.

Cell morphology analysis

The MH7A cells were seeded in 12-well plates (5 × 10^4 cells/well) and cultured for 24 hr before PDT treatment. After *in vitro* HYP-PDT treatment, medium was aspirated and cells were fixed with 4% paraformaldehyde for 5 min. Then, cells were washed twice with PBS and stained with or without 4′, 6-diamidino-2-phenylindole (DAPI) (Beyotime, Shanghai, China) for 5–10 min. Cell morphology was observed under a fluorescent microscope (Olympus, Japan) after three PBS washings.

Flow cytometry

MH7A cells were seeded in 6-well plates (1 × 10^5

cells/well). Irradiated cells were then harvested after HYP-PDT treatment. Live cells (Annexin V-FITC$^-$/PI$^-$), early apoptotic cells (Annexin V-FITC$^+$/PI$^-$), late apoptotic cells (Annexin V-FITC$^+$/PI$^+$) and necrotic cells (Annexin V-FITC$^-$/PI$^+$) were measured with FACS (Becton-Dickinson, Franklin Lakes, NJ, USA). Annexin V-FITC and PI apoptosis kits were purchased from BD Biosciences (Becton-Dickinson, Franklin Lakes, NJ, USA).

ROS assay

Intracellular ROSs were quantified using a commercial kit (Beyotime, Shanghai, China), following the manufacturer's instructions. Intracellular ROS production was evaluated by levels of oxidized dichlorofluorescein (DCF) from 2'7'-dichlorofluorescein diacetate (DCFH-DA) with probes; therefore, DCF is a proxy for intracellular ROS production. MH7A cells were seeded in 96-well plates (5×10^3 cells/well), and after HYP-PDT treatment, cells were incubated with DCFH-DA (10 μM) for 20 min at 37 °C in the dark, and then DCFH-DA was removed and cells were washed three times with DMEM/HIGH glucose without FBS. Absorbance of the cells was read on a plate reader at 488 nm (excitation) and 525 nm (emission).

Western blot

After HYP-PDT treatment, cells were washed three times with ice-cold PBS, and proteins were harvested using lysis buffer. Proteins were quantified using a BCA protein assay kit (Beyotime, Shanghai, China). Briefly, 20 μg protein was separated using 8–15% SDS-PAGE and transferred onto PVDF membranes. Blots were blocked with 10% instant nonfat dry milk at room temperature. Then, membranes were incubated with primary antibodies (1:1000 for all antibodies) overnight at 4 °C, and then incubated with secondary antibody for 2 hr. After washing three times with TBST, antibody binding was assayed with a gel imaging analysis system (Bio-Rad, Hercules, CA, USA). Relative intensities of protein bands were quantified by densitometry using ImageJ 1.50b software (NIH), and β-actin was used as an internal control.

Quantitative real-time PCR

After HYP-PDT treatment, cells were washed three times with ice-cold PBS. Total RNA was extracted using an RNAiso Plus Kit (TaKaRa, Tokyo, Japan) according to the manufacturer's instructions. Reverse transcription of extracted RNA was performed using a PrimeScript RT Reagent Kit (TaKaRa, Tokyo, Japan). Quantitative real-time PCR amplifications were executed using a rotor-gene real-time DNA amplification system (Corbett Research, Sydney, Australia). Relative fold-change in mRNA expression of the target gene was quantified using the $2^{-\Delta\Delta CT}$ method and Rotor-Gene 6.0 analysis software. *GAPDH* was used as internal control for all analyses. Primers used are presented in Table 1.

Statistical analysis

Data are assessed with SPSS Version 22 (IBM, Armonk, NY, USA), and expressed as means±SD. Differences among groups were analyzed with the LSD *post-hoc* test followed by one-way ANOVA, and $P<0.05$ was regarded as statistically significant difference, and significance was confirmed with Origin 9.0 software (Northampton, MA, USA).

Results

MH7A cell viability 24 hr post HYP-PDT

The impact of photocytotoxicity on MH7A cell viability following HYP treatment was examined. MTT assay data indicated that MH7A cell proliferation decreased in a dose dependent manner with light irradiation and with increasing doses of HYP (Figure 1A). Non-irradiated MH7A cell proliferation after treatment with HYP also decreased in a dose dependent manner, but not as significantly as HYP-PDT. This result suggested that HYP treatment can inhibit MH7A cell proliferation, an event that is exacerbated by PDT irradiation.

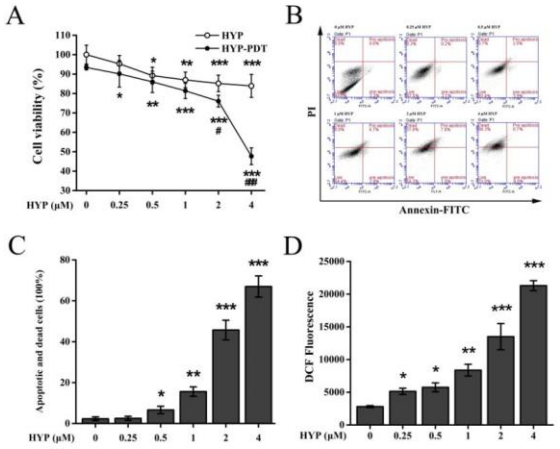

Figure 1. Effects of hypericin-photodynamic therapy on MH7A cell viability, apoptosis and production of intracellular reactive oxygen species. (A) Inhibition of cell viability by HYP-PDT was assayed using MTT. HYP-treated cells were subjected to PDT irradiation, and percent viable cells were normalized against untreated, non-irradiated cells (100%). Data are means±SD of n=5 independent experiments; *$P<0.05$, **$P<0.01$, ***$P<0.001$, compared to untreated, non-irradiated cells; $^{\#}P<0.05$, $^{\#\#}P<0.01$, $^{\#\#\#}P<0.001$, compared HYP-treated cells. (B, C) HYP-PDT induced apoptosis in MH7A cells. MH7A cells were treated with HYP (0–4 μM), and flow cytometry was used to measure apoptosis. HYP-PDT increased apoptosis and cell death in a concentration-dependent manner. Data are means±SD (n=3), *$P<0.05$, **$P<0.01$, ***$P<0.001$, compared with 0 μM HYP-PDT treated cells. (D) HYP-PDT enhanced ROS production in MH7A cells. Intracellular ROS production was measured using DCF 24 hr after treatment with increasing concentrations of HYP. DCF significantly increased with increasing HYP-PDT. With ≥1 μM HYP, DCF fluorescence increased and peaked with 4 μM HYP. Data were means ± SD (n = 3); *$P<0.05$, **$P<0.01$, ***$P<0.001$, compared to untreated cells (0 μM HYP)
DCF: dichlorofluorescein; HYP: hypericin; PDT: photodynamic therapy; ROS, reactive oxygen species

Table 1. Primers used for quantitative real-time polymerase chain reaction

Genes	Orientation	Primer sequence (5′ - 3′)
NF-κB	Forward	TTTGACCTGAGGGTAAGACTTCT
	Reverse	AACAGAGAGGATTTCGTTTCCG
GAPDH	Forward	GTTCGACAGTCAGCCGCATC
	Reverse	TGAAGGGGTCATTGATGGCA

Morphological changes of MH7A cells induced by HYP-PDT

To determine the impact of HYP concentrations on cell proliferation, an imaging analysis and DAPI staining assay were performed under a fluorescent microscope. Morphological alterations such as decrease in cell number, cytoplasmic vacuolation, and cytoplasm shrinkage were observed. As shown in Figure 2, cell number decreased significantly with increasing HYP concentration. Meanwhile, in morphological images, there was evidence of cytoplasmic vacuolation and shrinkage (Figure 2, white arrows), which were more obvious at the high HYP concentration (≥1 μM).

Additionally, the corresponding fluorescent merged images showed that cytoplasmic localization of HYP was displayed as bright red (Figure 2, white arrows in merged images) (18). Combined with results of MTT assay, these results showed that HYP was capable of permeating the membrane, inhibiting cell proliferation and inducing morphological changes that were indicative of cell death. Additionally, the effects of HYP in inhibiting cell proliferation were more prominent with higher HYP concentration (≥1 μM).

HYP-PDT induced apoptosis in MH7A cells

To confirm the HYP-PDT-induced apoptosis, flowcytometry was used to identify live cells (Annexin V-FITC$^-$/PI$^-$), early apoptotic cells (Annexin V-FITC$^+$/PI$^-$), late apoptotic cells (Annexin V-FITC$^+$/PI$^+$) and necrotic cells (Annexin V-FITC$^-$/PI$^+$). Figure 1B shows that apoptosis and cell death increased with increasing HYP and cell death was greatest observed at the highest dose (4 μM HYP) (Figure 1C). This result corresponded with the morphological changes assayed with the DAPI staining.

HYP-PDT enhanced intracellular ROS production in MH7A cells

To determine whether ROS generation contributed to apoptosis after HYP-PDT, the oxidation of the fluorescent probe DCFH-DA was used as a proxy of ROS production. Figure 1D shows that DCF fluorescence significantly increased after HYP-PDT in a concentration-dependent manner, with the highest fluorescence observed at the highest dose (4 μM) (P<0.01). Thus, HYP-PDT triggered accumulation of ROS in a dose-dependent manner.

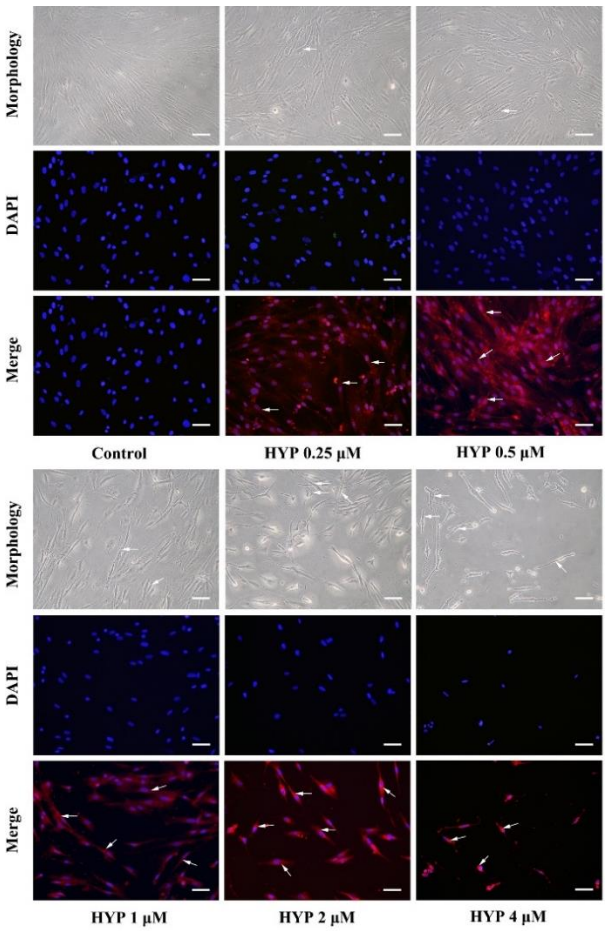

Figure 2. Morphological changes of MH7A cells induced by hypericin-photodynamic therapy. MH7A cells were pre-cultured with HYP (0, 0.25, 0.5, 1, 2 and 4 μM) for 1 hr in the dark and DAPI staining and fluorescent imaging was used to visualize morphology. Higher HYP (≥1 μM)-treated cells showed signs of cell death (reduced cell number, cytoplasmic vacuolation, and cytoplasm shrinkage; white arrows in morphology images). HYP was observed as bright red in the cytoplasm (white arrows in merge images). (200× magnification for all images; Scale bar is 50 μm)
HYP: hypericin; PDT: photodynamic therapy; DAPI: 4′, 6-diamidino-2-phenylindole

Effects of HYP-PDT on apoptosis pathway protein expression in MH7A cells

To identify the potential molecular mechanism underlying pro-apoptotic effects of HYP-PDT, we measured expression of several apoptosis pathway-related proteins using Western blot analysis. Figure 3A, C and E show that expression of full length caspase -8, caspase-9, and PARP was downregulated by HYP-PDT in a HYP concentration-dependent manner. In contrast, cleaved caspase-9 and cleaved PARP expression significantly increased with increasing concentrations of HYP. With increasing HYP, the cleaved caspase-9/caspase-9 ratio and cleaved PARP/PARP ratio was reduced (Figure 3B and D). Thus, HYP-PDT induced apoptosis, at least partially, through the intrinsic mitochondrial apoptosis pathway.

Although cleaved caspase-8 was not measured due

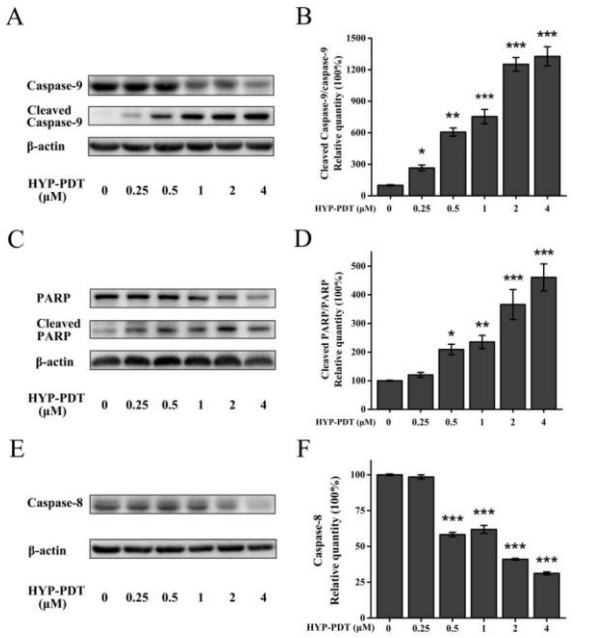

Figure 3. Effects of hypericin-photodynamic therapy on apoptosis pathway protein expression in MH7A cells. Cells were treated with HYP (0–4 μM) and then PDT irradiation. (A, C, E) Western blot was used to measure apoptotic proteins and β-actin was an internal control. Densitometric measurements were analyzed using ImageJ software. (B, D, F) Relative protein quantities were normalized against that of untreated cells (0 μM HYP; 100%). Graph bars represent means±SD from three independent experiments. *P<0.05, **P<0.01, ***P<0.001, compared to untreated cells (0 μM HYP)
HYP: hypericin; PDT: photodynamic therapy

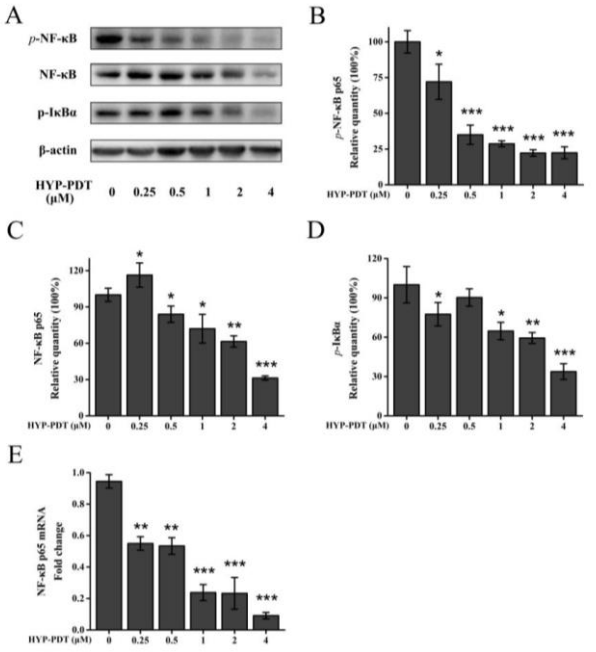

Figure 4. Inhibitory effects of hypericin-photodynamic therapy on NF-κB activation in MH7A cells. Cells were treated with HYP (0–4 μM) and PDT. NF-κB pathway proteins and mRNA were measured with Western blot and qRT-PCR, with β-actin used as an internal control. (A) Western blot data is shown for p-NF-κB p65, NF-κB p65 and p-IκBα and densitometric analysis performed using ImageJ software. Relative quantities of p-NF-κB p65 (B), NF-κB p65 (C) and p-IκBα (D) were normalized to untreated cells (0 μM HYP; 100%). (E) NF-κB p65 mRNA was assessed using qRT-PCR. Gene expression was normalized to GAPDH. Data are means±SD (n=3); ***P<0.001, compared to untreated cells (0 μM HYP)
HYP: hypericin; PDT: photodynamic therapy

to antibody quality, full length caspase-8 declined significantly in the presence of HYP ≥1 μM (Figure 3F). Nonetheless, downregulation of caspase-8 indicated that the extrinsic death receptor pathway may also be involved in HYP-PDT-induced apoptosis.

Inhibitory effects of HYP-PDT on NF-κB activation in MH7A cells

To determine whether NF-κB was involved in HYP-PDT-induced apoptosis, we measured p-NF-κB p65, NF-κB p65 and p-IκBα protein expression and NF-κB p65 mRNA. Figure 4A, B show that p-NF-κB p65 expression decreased with increasing HYP and p-IκBα declined in a dose-dependent manner with the exception for 0.5 μM HYP-treated cells, in which p-IκBα was less than in control cells (Figure 4D). Interestingly, NF-κB p65 expression with 0.25 μM HYP treatment significantly increased (Figure 4C), which was inconsistent with other results. Nonetheless, with HYP ≥ 0.5 μM, NF-κB p65 was downregulated in a concentration-dependent manner (Figure 4C). Figure 4E shows that NF-κB p65 mRNA decreased with increasing HYP. Thus, HYP ≥ 1 μM and PDT suppressed NF-κB activation in a dose-dependent manner, whereas the inhibitory effects of HYP-PDT on NF-κB activation varied with HYP at 0.25 μM or 0.5 μM.

Discussion

Recently, PDT has been shown to have potential for treating neoplastic diseases and RA (11, 30-33) as it can selectively induce necrosis or apoptosis of cancer cells, leaving healthy tissues and cells unaffected (12, 34). Meanwhile, HYP has been tested with PDT in tumor models *in vivo* and *in vitro*, and these confirmed that HYP-PDT had a light-induced antineoplastic activity against various tumors (35, 36). Also, HYP appears to have characteristics of high tumor affinity and is rapidly eliminated from normal tissue (10). However, whether HYP-PDT has a therapeutic effect on RA has not yet been investigated. RA is a systemic autoimmune disease characterized by inflammatory response and tumor-like synovial hyperplasia perhaps due to insufficient apoptosis of RA-FLS, which is similar to a locally invasive tumor (1). Hence, in this study, HYP-PDT was used to treat RA for the first time and the photocytotoxic effects of HYP were studied.

Our study indicated that HYP-PDT caused concentration-dependent photocytotoxic effects, especially at higher concentrations (≥1 μM). Figure 1A shows that HYP-PDT-treated cells had reduced viability than HYP-induced-cells without light irradiation treatment, indicating that the inhibitory effects of HYP was light-dependent.

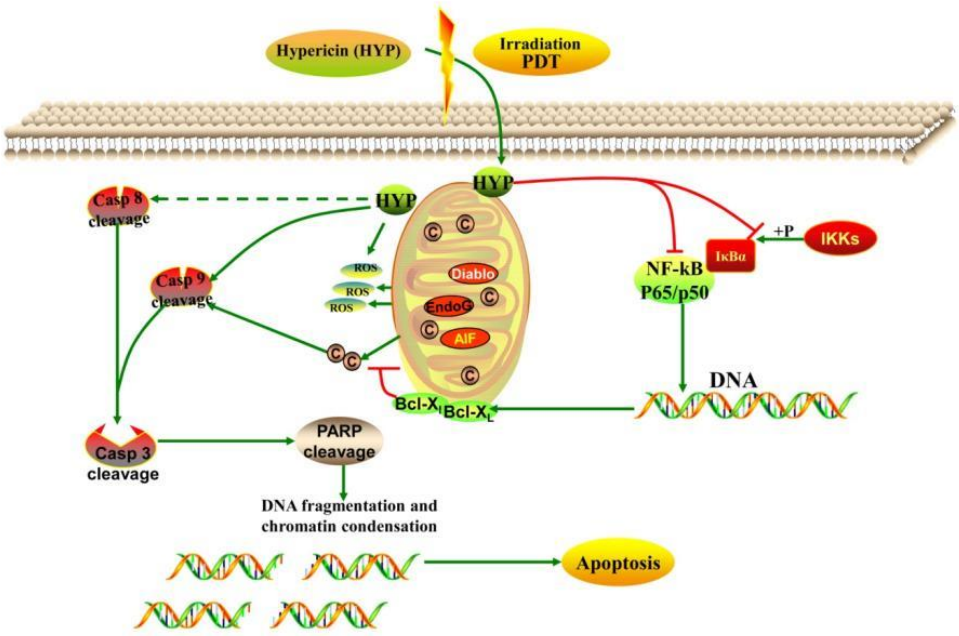

Figure 5. Proposed model of hypericin-photodynamic therapy-induced MH7A cell death. HYP assembles around target cells and permeates membranes *via* endocytosis, pinocytosis, or passive diffusion. HYP is bound to mitochondria and is activated after PDT irradiation and reacts with molecular oxygen to generate cytotoxic ROS, triggering cleavage of caspase, and initiating the caspase cascade. These events lead to apoptosis via activation of the intrinsic mitochondrial apoptosis pathway and suppression of the NF-κB pathway in MH7A cells. Additionally, the extrinsic death receptor pathway, which leads to activation of initiator caspase-8, may be involved in HYP-PDT-induced apoptosis. HYP, hypericin; PDT, photodynamic therapy; ROS, reactive oxygen species

Furthermore, HYP-PDT inhibited cell proliferation as shown by an imaging analysis and DAPI staining assay. With HYP ≥1 μM, we observed morphological features of cell death, such as reduced cell number, cytoplasmic vacuolation, and cytoplasmic shrinkage. Cells treated with HYP at 0.25 and 0.5 μM did not show distinctive morphological signs, which is consistent with the results of the MTT assay. Furthermore, flowcytometry demonstrated that HYP-PDT induced a pro-apoptotic effect on MH7A cells in a dose-dependent manner. The rate of apoptosis and cell death increased with increasing HYP concentration and this cell death was more pronounced at high HYP concentrations (≥1 μM). Because ROS is associated with apoptosis, the finding that HYP-PDT induced ROS strengthened the association of HYP-PDT with apoptosis (37, 38). Consequently, we found that HYP-PDT triggered ROS in a dose-dependent manner, and greater accumulation of ROS was observed at higher HYP doses (≥1 μM), especially in 2 μM and 4 μM HYP-treated group. In summary, our study confirmed that HYP-PDT induces apoptosis by triggering intracellular ROS production.

Excess ROS can promote mitochondrial toxicity, macromolecular membrane damage and DNA fragmentation by interacting with cellular DNA, proteins and lipids. ROS can also activate caspase signaling (39), consequently causing apoptosis (17, 40, 41). Therefore, we hypothesized that HYP-PDT-induced apoptosis may occur through the caspase apoptotic signaling pathway.

Two central caspase-dependent apoptotic pathways are involved in apoptosis: mitochondrial pathway (intrinsic), triggered by diverse cytotoxic conditions, leading to activation of initiator caspase-9; while the death receptor pathway (extrinsic) is triggered by TNF receptor aggregation on the plasma membrane, which leads to activation of initiator caspase-8. Subsequently, downstream effectors such as caspase-3 are activated by pre-activated caspase-8, and 9, and consequently PARP is cleaved, eventually triggering apoptosis. In this study, after HYP-PDT, full length caspase-9 and PARP were downregulated, whereas cleaved caspase-9 and cleaved PARP, as well as the cleaved caspase-9/caspase-9 ratio and the cleaved PARP/PARP ratio, significantly increased in a concentration-dependent manner. Meanwhile, full length caspase-8 declined, especially for cells treated with HYP ≥1 μM. This suggested that HYP-PDT induced apoptosis via the mitochondrial apoptotic pathway; the death receptor pathway may also be involved in pro-apoptotic effects of HYP-PDT.

NF-κB signaling pathway is critical to cell survival by upregulating the expression of anti-apoptosis genes and numerous target genes involved in cell growth, differentiation, and the inflammatory response (42-45). NF-κB is activated in many autoimmune diseases, including RA (46, 47), regulating inflammatory cytokines and modulating the resistance of RA-FLS against apoptosis (48-50). It has been demonstrated that NF-κB is a key molecule among the different transcription factors involved in modulating apoptosis of RA-FLS (51). NF-κB is represented mainly by the p65/p50 hetero-

dimeric complex. NF-κB is inactively bound to IκBα in the cytoplasm, and upon phosphorylation by IKKs, is released and translocated into the nucleus. Overexpression of NF-κB reduces secretion and expression of caspases via modulating Bcl-XL and apoptosis proteins/IAPs (52). Thus, we hypothesized that the NF-κB pathway may contribute to the underlying mechanism of pro-apoptotic effects of HYP-PDT in MH7A cells. Data showed that HYP-PDT inhibited NF-κB during MH7A cell apoptosis and that HYP decreased p-NF-κB p65, NF-κB p65, and p- IκBα in a concentration-dependent manner. Thus, HYP-PDT induced apoptosis by suppressing NF-κB activation.

Conclusion

HYP-PDT may have potential as a novel therapeutic strategy for treating human RA. However, these observations should be investigated in *in vivo* studies. Nonetheless, our data suggest a novel mechanism for HYP-PDT in relieving RA symptoms *in vitro*. Herein, we propose that upon cell permeation, HYP is bound to mitochondria and is activated upon PDT irradiation and generates cytotoxic ROS, triggering the caspase cascade. Both the intrinsic mitochondrial apoptosis pathway and the extrinsic death receptor pathway are subsequently activated leading to NF-κB inhibition in MH7A cells, and ultimately, apoptosis in MH7A cells.

Acknowledgment

The authors thank the sponsor: The Cultivation Project of Chinese Medicine Clinical Leading Talents of Henan Province (HNZYLJ201301009).

References

1. Firestein GS. Evolving concepts of rheumatoid arthritis. Nature 2003; 423:356-361.
2. Gabriel SE, Michaud K. Epidemiological studies in incidence, prevalence, mortality, and comorbidity of the rheumatic diseases. Arthritis Res Ther 2009; 11:229.
3. Gabriel SE. The epidemiology of rheumatoid arthritis. Rheum Dis Clin North Am 2001; 27:269-281.
4. Bartok B, Firestein GS. Fibroblast-like synoviocytes: key effector cells in rheumatoid arthritis. Immunol Rev 2010; 233:233-255.
5. Chen H, Pan J, Wang JD, Liao QM, Xia XR. Suberoylanilide hydroxamic acid, an inhibitor of histone deacetylase, induces apoptosis in rheumatoid arthritis fibroblast-like synoviocytes. Inflammation 2016; 39:39-46.
6. Baier A, Meineckel I, Gay S, Pap T. Apoptosis in rheumatoid arthritis. Curr Opin Rheumatol 2003; 15:274-279.
7. Pap T, Muller-Ladner U, Gay RE, Gay S. Fibroblast biology: Role of synovial fibroblasts in the pathogenesis of rheumatoid arthritis. Arthritis Res 2000; 2:361-367.
8. Lefevre S, Meier FM, Neumann E, Muller-Ladner U. Role of synovial fibroblasts in rheumatoid arthritis. Curr Pharm Des 2015; 21:130-141.
9. Jankowska A, Wiecek P, Burczynska B. Effect of photodynamic therapy on proliferation and apoptosis of 3T3 fibroblasts and HeLa cells. Photomed Laser Surg 2008; 26:343-347.
10. Torikai E, Kageyama Y, Kohno E, Hirano T, Koide Y, Terakawa S, *et al.* Photodynamic therapy using talaporfin sodium for synovial membrane from rheumatoid arthritis patients and collagen-induced arthritis rats. Clin Rheumatol 2008; 27:751-761.
11. Zhao C, Ur Rehman F, Yang Y, Li X, Zhang D, Jiang H, *et al.* Bio-imaging and Photodynamic therapy with tetra sulphonatophenyl porphyrin (TSPP)-TiO_2 nanowhiskers: new approaches in rheumatoid arthritis theranostics. Sci Rep 2015; 5:11518.
12. Byun JY, Choi HY, Myung KB, Choi YW. Expression of IL-10, TGF-beta(1) and TNF-alpha in cultured keratinocytes (HaCaT Cells) after IPL treatment or ALA-IPL photodynamic treatment. Ann Dermatol 2009; 21:12-17.
13. Agostinis P, Berg K, Cengel KA, Foster TH, Girotti AW, Gollnick SO, *et al.* Photodynamic therapy of cancer: an update. CA Cancer J Clin 2011; 61:250-281.
14. Lin XX, Wang W, Wu SF, Yang C, Chang TS. Treatment of capillary vascular malformation (port-wine stains) with photochemotherapy. Plast Reconstr Surg 1997; 99:1826-1830.
15. Gu Y, Huang NY, Liang J, Pan YM, Liu FG. Clinical study of 1949 cases of port wine stains treated with vascular photodynamic therapy (Gu's PDT). Ann Dermatol Venereol 2007; 134:241-244.
16. Luksiene Z, de Witte PA. Hypericin as novel and promising photodynamic therapy tool: studies on intracellular accumulation capacity and growth inhibition efficiency. Medicina (Kaunas) 2003; 39:677-682.
17. Barathan M, Mariappan V, Shankar EM, Abdullah BJ, Goh KL, Vadivelu J. Hypericin-photodynamic therapy leads to interleukin-6 secretion by HepG2 cells and their apoptosis via recruitment of BH3 interacting-domain death agonist and caspases. Cell Death Dis 2013; 4:e697.
18. Popovic A, Wiggins T, Davids LM. Differential susceptibility of primary cultured human skin cells to hypericin PDT in an *in vitro* model. J Photochem Photobiol B 2015; 149:249-256.
19. Kashef N, Karami S, Djavid GE. Phototoxic effect of hypericin alone and in combination with acetylcysteine on *Staphylococcus aureus* biofilms. Photodiagnosis Photodyn Ther 2015; 12:186-192.
20. Nakajima N, Kawashima N. A basic study on hypericin-PDT *in vitro*. Photodiagnosis Photodyn Ther 2012; 9:196-203.
21. Brockmoller J, Reum T, Bauer S, Kerb R, Hubner WD, Roots I. Hypericin and pseudohypericin: pharmacokinetics and effects on photosensitivity in humans. Pharmacopsychiatry 1997; 30 Suppl 2:94-101.
22. Lima AM, Pizzol CD, Monteiro FB, Creczynski-Pasa TB, Andrade GP, Ribeiro AO, *et al.* Hypericin encapsulated in solid lipid nanoparticles: phototoxicity and photodynamic efficiency. J Photochem Photobiol B 2013; 125:146-154.
23. Zhang J, Shao L, Wu C, Lu H, Xu R. Hypericin-mediated photodynamic therapy induces apoptosis of myeloma SP2/0 cells depended on caspase activity *in vitro*. Cancer Cell Int 2015; 15:58.
24. Xu Y, Wang D, Zhuang Z, Jin K, Zheng L, Yang Q, *et al.* Hypericin-mediated photodynamic therapy induces apoptosis in K562 human leukemia cells through JNK pathway modulation. Mol Med Rep 2015; 12:6475-6482.
25. Kleemann B, Loos B, Scriba TJ, Lang D, Davids LM. St John's Wort (*Hypericum perforatum* L.) photomedicine: hypericin-photodynamic therapy induces metastatic

melanoma cell death. PLoS One 2014; 9:e103762.
26. Li ZH, Meng DS, Li YY, Lu LC, Yu CP, Zhang Q, *et al.* Hypericin damages the ectatic capillaries in a Roman cockscomb model and inhibits the growth of human endothelial cells more potently than hematoporphyrin does through induction of apoptosis. Photochem Photobiol 2014; 90:1368-1375.
27. Miyazawa K, Mori A, Okudaira H. Establishment and characterization of a novel human rheumatoid fibroblast-like synoviocyte line, MH7A, immortalized with SV40 T antigen. J Biochem 1998; 124:1153-1162.
28. Zhang Q, Li ZH, Li YY, Shi SJ, Zhou SW, Fu YY, *et al.* Hypericin-photodynamic therapy induces human umbilical vein endothelial cell apoptosis. Sci Rep 2015; 5:18398.
29. Kammerer R, Buchner A, Palluch P, Pongratz T, Oboukhovskij K, Beyer W, *et al.* Induction of immune mediators in glioma and prostate cancer cells by non-lethal photodynamic therapy. PLoS One 2011; 6:e21834.
30. Krammer B, Verwanger T. Molecular response to hypericin-induced photodamage. Curr Med Chem 2012; 19:793-798.
31. Zheng Y, Yin G, Le V, Zhang A, Chen S, Liang X, *et al.* Photodynamic-therapy activates immune response by disrupting immunity homeostasis of tumor cells, which generates vaccine for cancer therapy. Int J Biol Sci 2016; 12:120-132.
32. Mirmalek SA, Azizi MA, Jangholi E, Yadollah-Damavandi S, Javidi MA, Parsa Y, *et al.* Cytotoxic and apoptogenic effect of hypericin, the bioactive component of Hypericum perforatum on the MCF-7 human breast cancer cell line. Cancer Cell Int 2015; 16:3.
33. Gabriel D, Busso N, So A, van den Bergh H, Gurny R, Lange N. Thrombin-sensitive photodynamic agents: a novel strategy for selective synovectomy in rheumatoid arthritis. J Control Release 2009; 138:225-234.
34. Fang N, Li Q, Yu S, Zhang J, He L, Ronis MJ, *et al.* Inhibition of growth and induction of apoptosis in human cancer cell lines by an ethyl acetate fraction from shiitake mushrooms. J Altern Complement Med 2006; 12:125-132.
35. Sanovic R, Verwanger T, Hartl A, Krammer B. Low dose hypericin-PDT induces complete tumor regression in BALB/c mice bearing CT26 colon carcinoma. Photodiagnosis Photodyn Ther 2011; 8:291-296.
36. Stupakova V, Varinska L, Mirossay A, Sarissky M, Mojzis J, Dankovcik R, *et al.* Photodynamic effect of hypericin in primary cultures of human umbilical endothelial cells and glioma cell lines. Phytother Res 2009; 23:827-832.
37. Simon HU, Haj-Yehia A, Levi-Schaffer F. Role of reactive oxygen species (ROS) in apoptosis induction. Apoptosis 2000; 5:415-418.
38. Zheng X, Wu J, Shao Q, Li X, Kou J, Zhu X, *et al.* Apoptosis of THP-1 macrophages induced by pseudohypericin-mediated sonodynamic therapy through the mitochondria-caspase pathway. Cell Physiol Biochem 2016; 38:545-557.
39. Green DR, Reed JC. Mitochondria and apoptosis. Science 1998; 281:1309-1312.
40. Bulina ME, Chudakov DM, Britanova OV, Yanushevich YG, Staroverov DB, Chepurnykh TV, *et al.* A genetically encoded photosensitizer. Nat Biotechnol 2006; 24:95-99.
41. Butler MC, Itotia PN, Sullivan JM. A high-throughput biophotonics instrument to screen for novel ocular photosensitizing therapeutic agents. Invest Ophthalmol Vis Sci 2010; 51:2705-2720.
42. Mitsiades CS, Mitsiades N, Poulaki V, Schlossman R, Akiyama M, Chauhan D, *et al.* Activation of NF-kappaB and upregulation of intracellular anti-apoptotic proteins via the IGF-1/Akt signaling in human multiple myeloma cells: therapeutic implications. Oncogene 2002; 21:5673-5683.
43. Hwang JR, Jo K, Lee Y, Sung BJ, Park YW, Lee JH. Upregulation of CD9 in ovarian cancer is related to the induction of TNF-alpha gene expression and constitutive NF-kappaB activation. Carcinogenesis 2012; 33:77-83.
44. Han SS, Yun H, Son DJ, Tompkins VS, Peng L, Chung ST, *et al.* NF-kappaB/STAT3/PI3K signaling crosstalk in iMyc E mu B lymphoma. Mol Cancer 2010; 9:97.
45. Barnes PJ, Karin M. Nuclear factor-kappaB: a pivotal transcription factor in chronic inflammatory diseases. N Engl J Med 1997; 336:1066-1071.
46. Pereira SG, Oakley F. Nuclear factor-kappaB1: regulation and function. Int J Biochem Cell Biol 2008; 40:1425-1430.
47. Vallabhapurapu S, Karin M. Regulation and function of NF-kappaB transcription factors in the immune system. Annu Rev Immunol 2009; 27:693-733.
48. Makarov SS. NF-kappa B in rheumatoid arthritis: a pivotal regulator of inflammation, hyperplasia, and tissue destruction. Arthritis Res 2001; 3:200-206.
49. Yin G, Wang Y, Cen XM, Yang M, Liang Y, Xie QB. Lipid peroxidation-mediated inflammation promotes cell apoptosis through activation of NF-kappaB pathway in rheumatoid arthritis synovial cells. Mediators Inflamm 2015; 2015:460310.
50. Aupperle KR, Bennett BL, Boyle DL, Tak PP, Manning AM, Firestein GS. NF-kappa B regulation by I kappa B kinase in primary fibroblast-like synoviocytes. J Immunol 1999; 163:427-433.
51. Karin M, Lin A. NF-kappaB at the crossroads of life and death. Nat Immunol 2002; 3:221-227.
52. Oeckinghaus A, Ghosh S. The NF-kappaB family of transcription factors and its regulation. Cold Spring Harb Perspect Biol 2009; 1:a000034.